HOKKAIDO UNIVERSITY

Title	Tumor endothelial cells with high aldehyde dehydrogenase activity show drug resistance
Author(s)	Hida, Kyoko; Maishi, Nako; Akiyama, Kosuke et al.
Citation	Cancer science, 108(11), 2195-2203 https://doi.org/10.1111/cas.13388
Issue Date	2017-11
Doc URL	https://hdl.handle.net/2115/67988
Rights(URL)	https://creativecommons.org/licenses/by-nc/4.0/
Type	journal article
File Information	Hida_et_al-2017-Cancer_Science.pdf

Hokkaido University Collection of Scholarly and Academic Papers : HUSCAP

Cancer Science
Japanese Cancer Association JCA
Open Access

Tumor endothelial cells with high aldehyde dehydrogenase activity show drug resistance

Kyoko Hida,[1,2,7] Nako Maishi,[1,2,7] Kosuke Akiyama,[1,2] Hitomi Ohmura-Kakutani,[1] Chisaho Torii,[1,2] Noritaka Ohga,[1] Takahiro Osawa,[3] Hiroshi Kikuchi,[1,3] Hirofumi Morimoto,[1,6] Masahiro Morimoto,[2] Masanobu Shindoh,[5] Nobuo Shinohara[3] and Yasuhiro Hida[4]

[1]Department of Vascular Biology, Hokkaido University Graduate School of Dental Medicine; [2]Vascular Biology, Institute for Genetic Medicine, Hokkaido University; [3]Department of Renal and Genitourinary Surgery, Graduate School of Medicine, Hokkaido University; [4]Department of Cardiovascular and Thoracic Surgery, Hokkaido University Graduate School of Medicine; [5]Department of Oral Pathology and Biology, Hokkaido University Graduate School of Dental Medicine; [6]Department of Gastroenterological Surgery II, Graduate School of Medicine, Hokkaido University, Sapporo, Japan

Key words

Aldehyde dehydrogenase (ALDH), angiogenesis, endothelial cell, resistance, tumor

Correspondence

Kyoko Hida, Vascular Biology, Frontier Research Unit, Institute for Genetic Medicine, Hokkaido University, N15 W7, Kita-ku, Sapporo 060-0815, Japan.
Tel: +81-11-706-4315; Fax: +81-11-706-4325;
E-mail: khida@igm.hokudai.ac.jp

[7]These authors contributed equally to this work.

Funding Information

Supported by Grants-in-Aid for Scientific Research from the Ministry of Education, Science, and Culture of Japan (grant 23112501 to K.H.) and Kobayashi Foundation for Cancer Research (K.H.).

Received April 7, 2017; Revised August 11, 2017; Accepted August 16, 2017

Cancer Sci **108** (2017) 2195–2203

doi: 10.1111/cas.13388

Tumor blood vessels play an important role in tumor progression and metastasis. We previously reported that tumor endothelial cells (TEC) exhibit several altered phenotypes compared with normal endothelial cells (NEC). For example, TEC have chromosomal abnormalities and are resistant to several anticancer drugs. Furthermore, TEC contain stem cell-like populations with high aldehyde dehydrogenase (ALDH) activity (ALDH^{high} TEC). ALDH^{high} TEC have proangiogenic properties compared with ALDH^{low} TEC. However, the association between ALDH^{high} TEC and drug resistance remains unclear. In the present study, we found that ALDH mRNA expression and activity were higher in both human and mouse TEC than in NEC. Human NEC:human microvascular endothelial cells (HMVEC) were treated with tumor-conditioned medium (tumor CM). The ALDH^{high} population increased along with upregulation of stem-related genes such as multidrug resistance 1, CD90, ALP, and Oct-4. Tumor CM also induced sphere-forming ability in HMVEC. Platelet-derived growth factor (PDGF)-A in tumor CM was shown to induce ALDH expression in HMVEC. Finally, ALDH^{high} TEC were resistant to fluorouracil (5-FU) *in vitro* and *in vivo*. ALDH^{high} TEC showed a higher grade of aneuploidy compared with that in ALDH^{low} TEC. These results suggested that tumor-secreting factor increases ALDH^{high} TEC populations that are resistant to 5-FU. Therefore, ALDH^{high} TEC in tumor blood vessels might be an important target to overcome or prevent drug resistance.

Antiangiogenic therapy is a valuable strategy for cancer treatment and it prolongs the survival of patients with certain cancer types.[1] The advantage of targeting EC instead of tumor cells is that unlike tumor cells, ECs are genetically stable and do not develop drug resistance.[2,3] However, resistance to this therapy has been reported.[4,5] The major mechanism involved in developing resistance is tumor cell phenotypic change. For example, tumor cells express other angiogenic factors in response to the inhibition of certain factors.[6] Stromal cells, besides tumor cells, are occasionally involved in the development of resistance. We previously compared the characteristics of TEC and NEC and found that TEC contain several abnormalities such as specific upregulated genes[7–10] and cytogenetic abnormalities.[11,12]

We also demonstrated expression of stem cell markers such as MDR1, a well-known stem cell marker and an ABC transporter.[13] In addition, TEC form spheres and have a differentiation ability for osteoblasts.[14] We also focused on ALDH, another stem cell marker, that plays a key role in aldehyde metabolism. Several stem cell types, including hematopoietic stem cells[15] and neural stem cells,[16] possess high ALDH activities. We found that ALDH was upregulated in TEC compared with that in NEC.[17] We isolated ALDH^{high} TEC and ALDH^{low} TEC and reported that ALDH^{high} TEC are more proangiogenic compared with ALDH^{low} TEC. In addition, a side population of EC with ABC transporter gene upregulation is present in blood vessels.[18] These results suggest that stem-like cells exist in tumor blood vessels. Furthermore, TEC that express Pgp demonstrate resistance to antiangiogenic drugs.[19] We also reported that TEC are resistant to paclitaxel by Pgp upregulation.[13,20] ALDH is highly expressed in cancer stem cells, which contributes to drug resistance. However, the role of ALDH^{high} TEC in drug resistance remains unknown. The present study aimed to investigate the role of ALDH^{high} TEC in the development of drug resistance.

Materials and Methods

Mice. Six-week-old female nude mice (BALB/c AJcl-nu/nu; Clea, Tokyo, Japan) were housed under specific pathogen-free conditions. All procedures for animal care and experimentation adhered to institutional guidelines and were approved by the Hokkaido University Animal Committee.

Human tissue samples. Tumor tissues were surgically excised from patients who were clinically diagnosed as having RCC.

© 2017 The Authors. *Cancer Science* published by John Wiley & Sons Australia, Ltd on behalf of Japanese Cancer Association.
This is an open access article under the terms of the Creative Commons Attrib ution-NonCommercial License, which permits use, distribution and reproduction in any medium, provided the original work is properly cited and is not used for commercial purposes.

When possible, normal renal tissues were separated from tumor tissues of the same patients. A portion of the tissue samples was immediately snap frozen in liquid nitrogen and stored at −80°C for immunohistochemistry. Another portion was placed in HBSS (Thermo Fisher Scientific, Waltham, MA, USA) on ice until EC isolation. Final diagnosis of RCC was confirmed on the basis of pathological examination of formalin-fixed surgical specimens. All protocols were approved by the Institutional Ethics Committee of Hokkaido University, and written informed consent was obtained from each patient before surgery.

Cells and culture conditions. HMVEC were obtained from Lonza (Tokyo, Japan) and cultured EGM-2MV. Super-metastatic human melanoma (A375SM) cells, a kind gift from Dr Isaiah J. Fidler (MD Anderson Cancer Center, Houston, TX, USA), were cultured in MEM (Thermo Fisher Scientific) supplemented with 10% heat-inactivated FBS. mTEC were isolated from tumors that were s.c. xenografted with A375SM. mNEC were isolated from the dermis of tumor-free nude mice as previously described.[11] hTEC and hNEC were isolated from tumor tissues and corresponding normal renal tissues, respectively, in RCC patients as previously described.[12] In brief, EC were isolated using a magnetic cell sorter device (Miltenyi Biotec, Bergisch Gladbach, Germany) and flow cytometry (FACS Aria II; BD Biosciences, San Jose, CA, USA) using an anti-CD31 antibody after removing leukocytes with an anti-CD45 antibody. CD31-positive cells were sorted and seeded on 1.5% gelatin-coated culture plates with EGM-2MV medium containing 15% FBS. For mouse EC isolation, diphtheria toxin (500 ng/mL; Calbiochem, San Diego, CA, USA) was added to the TEC subcultures to eliminate the remaining human tumor cells and NEC subcultures for technical consistency. Subcultured EC were sorted by a second round of purification using FITC-conjugated *Bandeiraea simplicifolia* lectin isolectin B4 (Vector Laboratories, Burlingame, CA, USA) for mouse EC and fluorescein *Ulex europaeus* agglutinin I (Vector Laboratories) for human EC. Cells were cultured at 37°C in a humidified atmosphere containing 5% CO_2.

Antibodies. The following antibodies were used: purified rat anti-mouse CD31 antibody (BD Pharmingen), Alexa 647-conjugated anti-mouse CD31 antibody, APC-conjugated anti-mouse CD45 antibody, purified mouse anti-human CD31 antibody, Alexa 647-conjugated anti-human CD31 antibody, PE-conjugated anti-human CD45 antibody (BioLegend, San Diego, CA, USA), anti-ALDH1A1 antibody (Abcam, Cambridge, UK), Alexa 594-conjugated anti-rabbit IgG, and Alexa Fluor 568-conjugated anti-rat IgG antibody (Invitrogen, Tokyo, Japan).

RT-PCR and real-time RT-PCR. Total RNA was extracted from each type of EC using the ReliaPrep RNA Cell Miniprep System (Promega, Madison, WI, USA). First-strand cDNA was synthesized using ReverTra-Plus (Toyobo Co., Osaka, Japan). Real-time RT-PCR was carried out using the KAPA SYBR Fast qPCR Kit (Nippon Genetics, Tokyo, Japan). Cycling conditions followed the manufacturer's instructions, and the CFX Manager (Bio-Rad, Hercules, CA, USA) was used for analysis. Expression levels were normalized to GAPDH levels and were analyzed using the delta-delta-Ct method. The primers used were as follows:

mouse GAPDH: forward, 5′-TCTGACGTGCCGCCTGGAG-3′, reverse, 5′-TCGCAGGAGACAACCTGGTC-3′; human GAPDH: forward, 5′-ACAGTCAGCCGCATCTTCTT-3′, reverse, 5′-GCCCAATACGACCAAATCC-3′; mouse ALDH: forward, 5′-TCCGTCATGACCACCAGGTGCTTTCC-3′, reverse, 5′-ACAACACCTGGGGAACAGAGCAG-3′; human ALDH: forward, 5′-TGTTAGCTGATGCCGACTTG-3′, reverse, 5′-TTCTTAGCCCGCTCAACACT-3′; human MDR1: forward, 5′-TGATTGCATTTGGAGGACAA-3′, reverse, 5′- ACCAGAAGGCCAGAGCATAA-3′; human ALP: forward, 5′-CCTCCTCGGAAGACACTCTG-3′, reverse, 5′- GCAGTGAAGGGCTTCTTGTC-3′; human Oct4: forward, 5′-TGCAGCAGATCAGCCACATCGC-3′, reverse, 5′- AGTCGCTGCTTGATCGCTTGCC-3′; human CD90: forward, 5′-CTAGTGGACCAGAGCCTTCG-3′, reverse, 5′- TGGAGTGCACACGTGTAGGT-3′.

Immunohistochemistry. Mouse tumor tissues were dissected from A375SM melanoma xenografts in nude mice. Human tissue samples were obtained from excised RCC and normal kidney tissues of patients. Tumor specimens embedded in Tissue-Tek OCT compound (Sakura Finetek Japan, Tokyo, Japan) were immediately immersed in liquid nitrogen and cut into sections using a cryotome. The frozen sections were fixed in 4% paraformaldehyde for 10 min and then blocked with 2% goat and 5% sheep sera in PBS for 1 h. Mouse sections were double stained with primary anti-ALDH1A1 and Alexa 647-conjugated anti-mouse CD31 antibodies. Human sections were double stained with anti-ALDH1A1 and Alexa 647-conjugated anti-human CD31 antibodies. All immunostained samples were counterstained with DAPI (Roche Diagnostics, Mannheim, Germany) and visualized under a FV1000 confocal microscope (Olympus, Tokyo, Japan). The acquired images were processed using Fluoview FV10-ASM Viewer software (Olympus). CD31-positive areas were demarcated using Image J software (National Institutes of Health), and these areas, as a percentage of the total area, were used as MVD.

Preparation of tumor-conditioned medium. A375SM cells were seeded and cultured in MEM supplemented with 10% FBS until 70%–80% confluence. Subsequently, the culture medium was replaced with fresh medium. After 18–20 h of incubation, the culture supernatant was collected as tumor CM and passed through a 0.22-μm filter (Millipore, Billerica, MA, USA) to eliminate the cells. HMVEC were exposed to fresh CM for 5 days, with CM changed after 2 days. For the control, HMVEC were incubated for 18–20 h in MEM supplemented with 10% FBS, and HMVEC CM was collected as described above.

Flow cytometric analyses of ALDH activity and isolation of ALDH^{high} TEC and ALDH^{low} TEC. An ALDEFLUOR kit (StemCell Technologies, Durham, NC, USA) was used according to the manufacturer's instructions to analyze ALDH enzymatic activity and to isolate the cell population with high ALDH activity. Cells were suspended in ALDEFLUOR assay buffer containing the ALDH substrate BAAA and incubated for 40 min at 37°C. BAAA was taken up by live cells and converted into BODIPY-aminoacetate by intracellular ALDH, yielding bright fluorescence. As the negative control, cells were stained under identical conditions with the specific ALDH inhibitor, diethylaminobenzaldehyde. The ALDH^{high} TEC and ALDH^{low} TEC populations were detected and sorted using FACS Aria II (BD Biosciences) with a 488-nm blue laser and standard FITC 530/30-nm bandpass filter.

Stemness spheroid assay. A cell suspension was seeded in a 96-well plate containing a microsphere array chip (STEM Biomethod; KSRP, Kitakyusyu, Japan), and 20 cells were seeded into microwells containing the culture medium, according to the manufacturer's instructions. Spheroids were observed using an inverted microscope (CKX41; Olympus).

ELISA. PDGF-A concentrations in tumor CM and control CM were determined by using PDGF ELISA (R&D Systems,

© 2017 The Authors. *Cancer Science* published by John Wiley & Sons Australia, Ltd on behalf of Japanese Cancer Association.

Minneapolis, MN, USA), according to the manufacturer's instructions.

Anticancer drug treatment in tumor-bearing mice. A375SM cells (1×10^6) were s.c. implanted in the right flanks of nude mice. When tumors reached an average size of 200 mm^3, mice were treated with sterile HBSS (i.p. twice weekly, control) or low-dose metronomic 5-FU (10 mg/kg i.p. twice weekly). For these experiments, 3–4 mice per group were used. Mice were regularly monitored. After 37 days of treatment, the tumors were excised. Mice were killed, and tumor tissues were processed for histological analysis.

Cell survival assay. For analyzing cell sensitivity to 5-FU, the dead cell population was analyzed using FACS Aria II with the Annexin V-FLUOS staining kit (Roche, Basel, Switzerland) after $ALDH^{high}$ TEC and $ALDH^{low}$ TEC were treated with 5-FU (1 μM) for 72 h. ALDH mRNA knockdown using siRNA was carried out to investigate ALDH contribution in 5-FU resistance in TEC. ALDH siRNA was sense: AGGCACUCAAUGGUGG-GAAAGUCUU, antisense: AAGACUUUCCCACCAUUGA-GUGCCU (Thermo Fisher Scientific). After transfection with ALDH siRNA, TEC were seeded in EBM-2 containing 0.5% FBS. Cell proliferation was measured daily for 3 days using the 3-(4,5-dimethylthylthiazol-2-yl)-5-(3-carboxymethoxyphenyl)-2-(4-sulfophenyl)-2H-tetrazolium (MTS) assay (Promega) in the presence of each 5-FU concentration.

Cell cycle analysis. $ALDH^{high}$ TEC and $ALDH^{low}$ TEC were prepared for analysis as described in the instructions provided with the Cycletest Plus DNA Reagent Kit (BD Biosciences). Following staining of cells with PI solution for 30 min, distribution of cells across different cell cycle phases was analyzed using the DNA histograms obtained using FACS Aria-II and FlowJo software (Ashland, TreeStar, OR, USA).

FISH. $ALDH^{high}$ TEC and $ALDH^{low}$ TEC were cytospun onto slides and the samples were fixed for 45 min using Histochoice (AMRESCO, Solon, OH, USA), as previously described.[11] FISH was carried out using a Cy3-mouse chromosome-17 locus-specific A1 probe (RP23-146B6; Chromosome Science, Sapporo, Japan) as described previously.[21] All samples were counterstained with DAPI. Hybridization signals were observed and analyzed using an Olympus IX71 fluorescence microscope (Olympus). Chromosomes were counted in at least 100 interphase nuclei for each sample. Aneuploid cells were counted three times in each sample. Cells with a single signal for each probe were not included in the analysis because

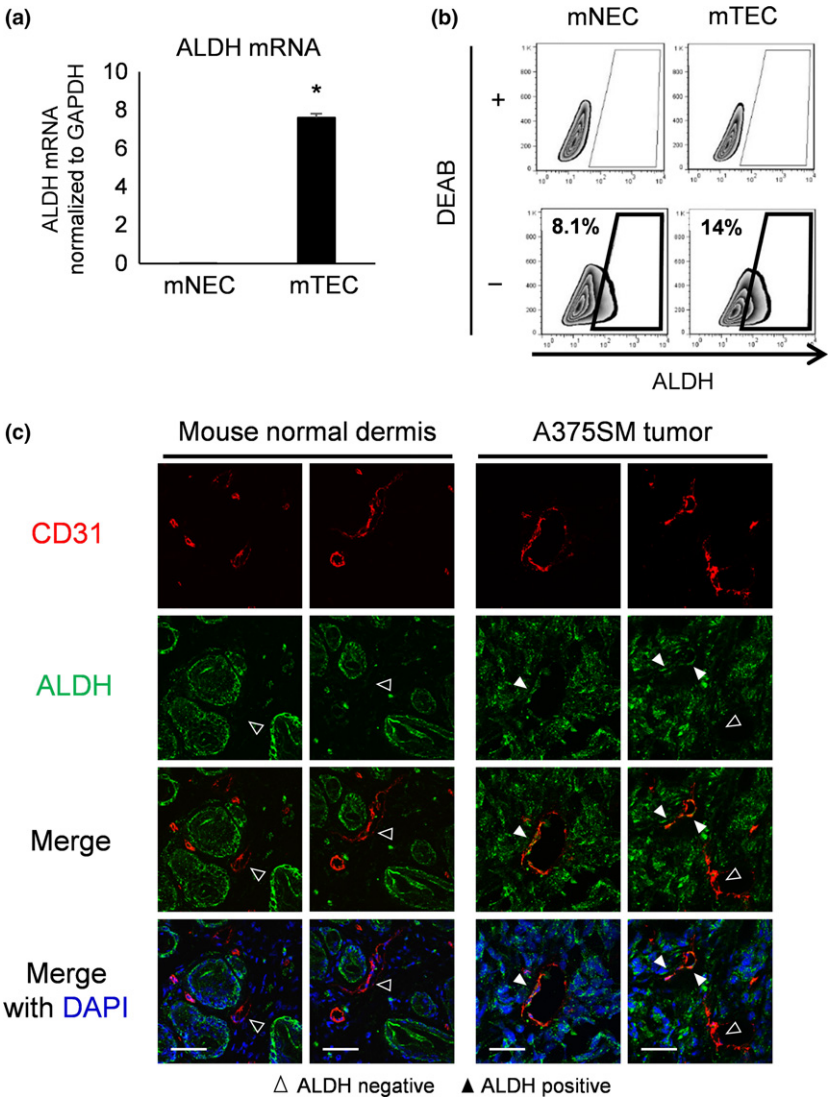

Fig. 1. Expression of aldehyde dehydrogenase (ALDH) in mouse tumor endothelial cells (TEC). (a) ALDH mRNA was analyzed in mouse TEC (mTEC) and mouse normal EC (mNEC) using real-time RT-PCR (*$P < 0.01$). (b) ALDH activity was measured in mTEC and mNEC using flow cytometry and the ALDEFLUOR kit (StemCell Technologies, Durham, NC, USA). DEAB is a specific ALDH inhibitor. Percentage of tumor endothelial cell containing stem-like populations with high ALDH activity ($ALDH^{high}$ TEC) is shown. (c). Double immunofluorescence staining for endothelial marker CD31 and ALDH in normal mouse tissue (dermis) and super-metastatic human melanoma (A375SM) xenografts. Merged image (DAPI) shows colocalization of ALDH (green) and CD31. Triangles show ALDH-negative endothelial cells, whereas arrowheads point to ALDH-positive endothelial cells. Scale bar, 50 μm.

© 2017 The Authors. *Cancer Science* published by John Wiley & Sons Australia, Ltd on behalf of Japanese Cancer Association.

it was difficult to determine whether the single signal was as a result of monosomy or incomplete hybridization.

Statistical analysis. Unless otherwise specified, all data are expressed as the mean ± standard deviation. Differences among groups were determined using one-way ANOVA, followed by a Tukey–Kramer multiple comparison test. A two-sided Student's *t*-test was used for comparison between two groups. *P*-value <0.05 was considered to be significant, and that of <0.01 was considered to be highly significant.

Results

ALDH expression in mouse TEC. TEC were isolated from A375SM xenografts in nude mice, and NEC were isolated from the dermis of normal nude mice, as previously reported. Cells were characterized in terms of EC phenotype and used in the experiments.[11]

Aldehyde dehydrogenase is a stem cell marker that is extensively used as a marker of hematopoietic stem cells and neural stem cells.[16] Furthermore, recent studies have identified ALDH enzymatic activity as a potential marker for cancer stem cells.[22] We previously reported that TEC expressed higher ALDH levels compared with NEC.[17] Consistent with the previous report, ALDH mRNA expression levels in TEC were significantly higher than those in NEC (Fig. 1a). ALDH activity assays revealed that the ALDH activity of TEC was higher than that of NEC. A representative analysis showed that 14% of TEC were ALDH^{high} cells, whereas only 8.1% of NECs were ALDH^{high} cells (Fig. 1b).

To analyze ALDH expression in tumor blood vessels *in vivo*, immunofluorostaining was carried out using anti-CD31 and anti-ALDH antibodies. In the normal dermis of mice, ALDH was not stained in CD31-positive blood vessels. However, ALDH was strongly stained in several A375SM tumor blood vessels, indicating the presence of ALDH^{high} TEC *in vivo* (Fig. 1c).

ALDH expression in human TEC. We also examined ALDH expression in human TEC. Although not expressed in human

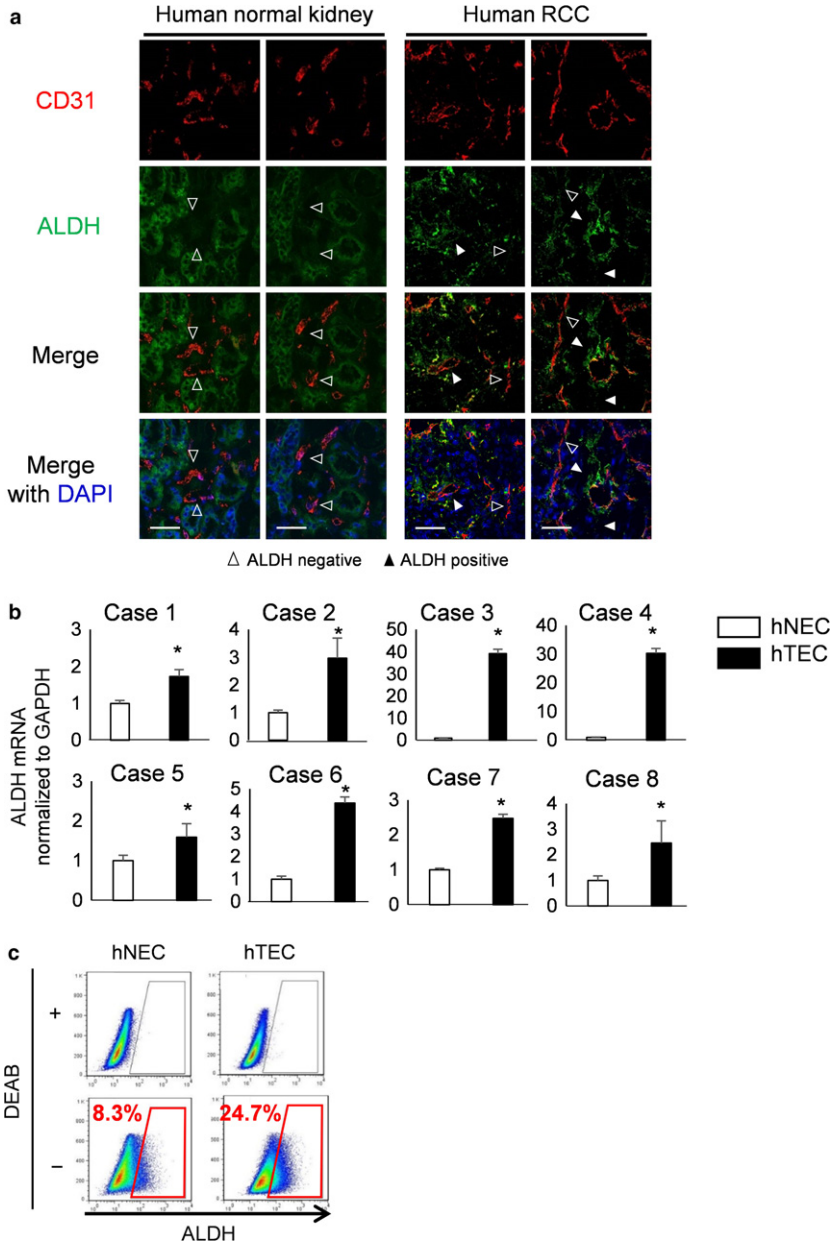

Fig. 2. Expression of aldehyde dehydrogenase (ALDH) in human tumor endothelial cells (TEC). (a) Double immunofluorescence staining for endothelial marker CD31 (red) and ALDH (green) in human normal kidney tissues and human renal cell carcinoma (RCC). Triangles show ALDH-negative endothelial cells, whereas arrowheads point to ALDH-positive endothelial cells. Scale bar, 50 μm. (b) ALDH mRNA expression was compared between human normal EC (hNEC) and human TEC (hTEC) isolated from non-cancerous tissue and RCC tissue, respectively (eight patients) using real-time RT-PCR (*$P < 0.01$). (c) ALDH activity was analyzed in hNEC and hTEC using flow cytometry and the ALDEFLUOR kit (StemCell Technologies, Durham, NC, USA).

© 2017 The Authors. *Cancer Science* published by John Wiley & Sons Australia, Ltd on behalf of Japanese Cancer Association.

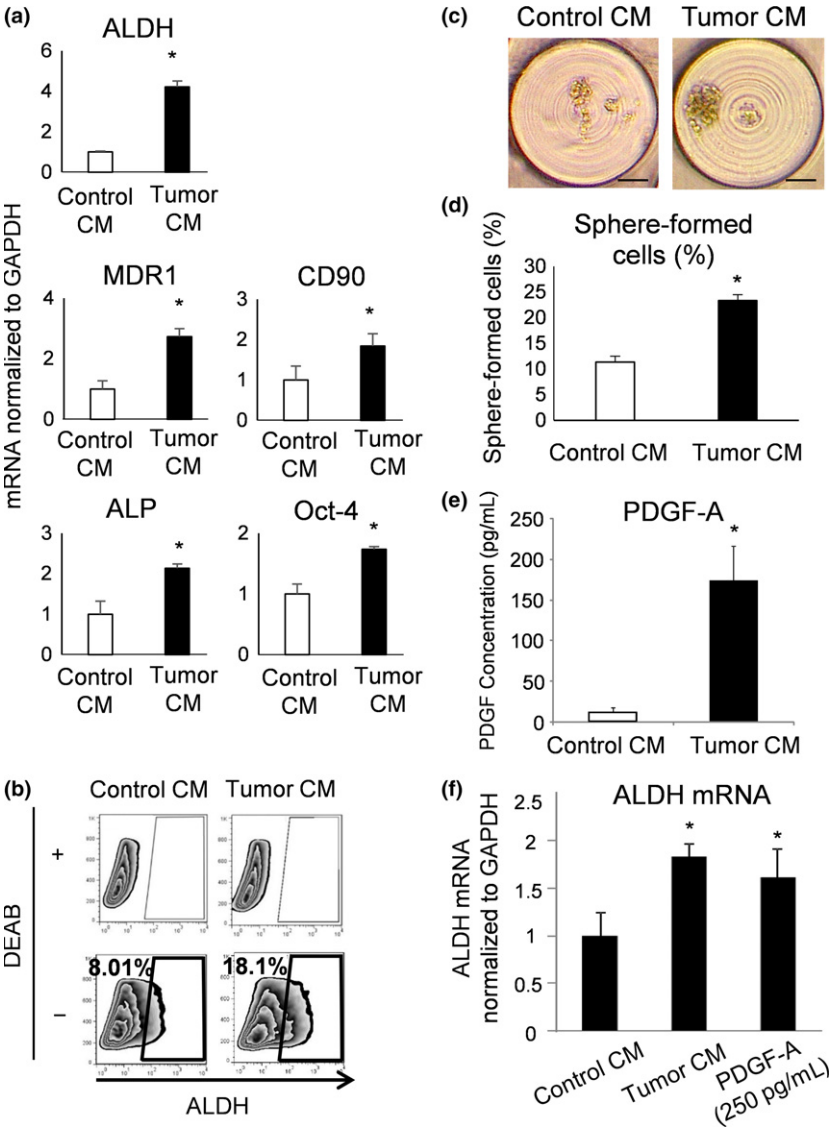

Fig. 3. Induction of stem-like phenotype by tumor-conditioned medium (CM). (a) Expression of aldehyde dehydrogenase (ALDH), MDR1, CD90, ALP, and Oct-4, normalized to GAPDH, was measured in human microvascular endothelial cells (HMVEC) after tumor CM treatment using real-time RT-PCR (*$P < 0.01$). (b) ALDH activity was analyzed using flow cytometry after treatment with tumor CM for 24 h. Proportion of high ALDH activity tumor endothelial cells (ALDH^{high} TEC) was measured and counted. (c) HMVEC were photographed at 72 h after seeding into microwells that contained culture medium. Of note, HMVEC treated with tumor CM showed spheroid morphology with a smooth surface and high circularity. Scale bars, 50 μm. (d). Number of sphere-forming cells in HMVEC treated with control CM or tumor CM (*$P < 0.05$). (e) Platelet-derived growth factor (PDGF)-A concentration was determined in control CM and tumor CM (*$P < 0.01$). (f) HMVEC were treated by tumor CM or PDGF-A. ALDH expression was determined by real-time RT-PCR (*$P < 0.01$).

normal kidney blood vessels, ALDH-positive tumor blood vessels in human RCC were observed (Fig. 2a). hNEC and hTEC were isolated from non-cancerous and cancerous regions of clinically dissected RCC specimens, respectively. Consistent with mouse EC, ALDH mRNA levels were significantly greater in hTEC than in hNEC (Fig. 2b). ALDH activity assays revealed that the ALDH activity of hTEC was also higher than that of hNEC. A representative analysis showed that 24.7% of TEC were ALDH^{high} cells, whereas only 8.3% of NEC were ALDH^{high} cells (Fig. 2c).

Tumor-secreting factor induced stem cell-like phenotype in EC. To examine the involvement of tumor-secreting factor in TEC stem cell-like phenotype, human NEC (HMVEC) were treated with tumor CM. mRNA ALDH, MDR1, CD90, ALP, and Oct-4 levels were elevated in HMVEC by 24-h treatment of tumor CM (Fig. 3a). ALDH activity was also enhanced in tumor CM-treated HMVEC compared with control CM-treated HMVEC (18.1% and 8.01%, respectively) (Fig. 3b).

In addition, tumor CM-treated HMVEC showed spheroid morphology with a smooth surface and high circularity at 72 h after seeding the cells onto a microchip (Fig. 3c). The number of sphere-forming cells in tumor CM-treated HMVECs was significantly higher than that in control CM-treated HMVECs (Fig. 3d).

Next, we investigated the mechanism underlying the induction of ALDH expression by tumor CM. STAT3 was reported to play important roles in ALDH-positive cancer stem cells[23] and, therefore, we focused on STAT3-activating growth factors. Tumor CM was shown to contain higher PDGF-A levels compared with those in the control CM (Fig. 3e). PDGF-A was shown to upregulate ALDH expression in HMVEC, like tumor CM (Fig. 3f).

ALDH^{high} TEC are resistant to 5-FU. ALDH is reportedly upregulated in cancer stem cells, which causes resistance to cancer therapy. We previously reported that TEC are also resistant to anticancer drugs.[13] Thus, we hypothesized that ALDH^{high} TEC are involved in drug resistance in TEC. To address this hypothesis, ALDH^{high} TEC and ALDH^{low} TEC were isolated using flow cytometry (Fig. 4a). After confirming ALDH mRNA in isolated ALDH^{high} TEC and ALDH^{low} TEC (Fig. 4b), TEC were treated with 1 μM 5-FU for 72 h, and a PI annexin assay was carried out. Dead ALDH^{high} TEC were fewer than dead ALDH^{low} TEC (Fig. 4c,d), indicating 5-FU resistance. Furthermore, to assess the resistance of ALDH^{high}

© 2017 The Authors. *Cancer Science* published by John Wiley & Sons Australia, Ltd on behalf of Japanese Cancer Association.

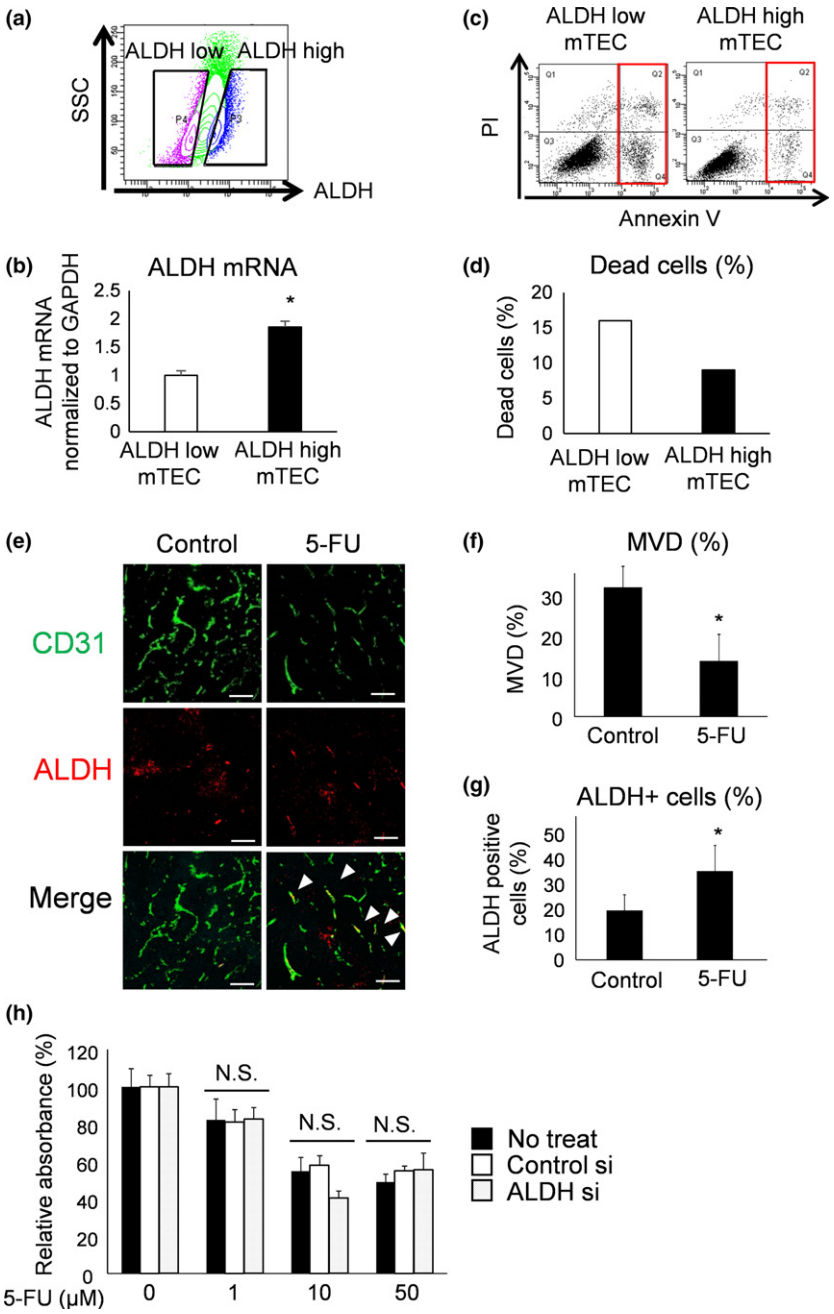

Fig. 4. High aldehyde dehydrogenase activity tumor endothelial cells (ALDH^{high} TEC) show resistance to fluorouracil (5-FU). (a) ALDH^{high} TEC and low ALDH activity TEC (ALDH^{low} TEC) in the indicated gates were sorted using FACS Aria II (BD Biosciences, San Jose, CA, USA). (b) ALDH mRNA levels were analyzed using real-time RT-PCR in the sorted ALDH$^{high/low}$ TEC (*$P < 0.01$). (c) The dead cell population treated with 5-FU was analyzed using flow cytometry as detected for propidium iodide (PI)- or annexin V-positive cells (red box). (d) Percentages of dead cells were compared between ALDH^{high} TEC and ALDH^{low} TEC (*$P < 0.01$). (e) Double immunofluorescence staining for endothelial marker CD31 (green) and ALDH (red) in super-metastatic human melanoma (A375SM) tumor tissues following injection of vehicle (control) or 5-FU. White arrowheads show ALDH and CD31-double-positive blood EC. Scale bar, 200 μm. (f) Microvessel density (MVD) was calculated from the CD31-positive area as a percentage of the total area by Image J in control- and 5-FU-treated tumors. $n = 5$ (*$P < 0.01$). (g) Percentage of ALDH-positive cells in the total CD31-positive cells was calculated using Image J in control- and 5-FU-treated tumors. $n = 5$ (*$P < 0.01$). (h) Sensitivity to 5-FU in ALDH siRNA-transfected TEC was compared with that of control siRNA-transfected TEC and non-treated TEC by the MTS assay. N.S., not significant.

TEC *in vivo,* low-dose 5-FU was applied in a metronomic schedule (targeting tumor blood vessels) to A375SM tumor-bearing mice. After treatment, tumor tissues were dissected from mice and examined using immunofluorostaining with anti-CD31 and anti-ALDH antibodies (Fig. 4e). MVD was significantly decreased in the 5-FU-treated group, suggesting that treatment inhibited angiogenesis (Fig. 4e CD31 staining, Fig. 4f). Conversely, the ALDH-positive blood vessel (ALDH+/CD31 +) population (Fig. 4e white arrowheads) significantly increased in the 5-FU-treated group compared with that in the control group (Fig. 4g). These results suggest that ALDH^{high} TEC are resistant to 5-FU *in vivo*, consistent with *in vitro* results. To evaluate the involvement of ALDH in developing resistance to 5-FU, ALDH knockdown by siRNA was carried out in TEC. The MTS assay showed that ALDH knockdown did not change the sensitivity to 5-FU, suggesting that ALDH expression is not directly linked to drug resistance in TEC (Fig. 4h).

ALDH^{high} TEC show a higher grade of aneuploidy. We previously demonstrated that ALDH^{high} TEC have a lower proliferation rate compared with that of the ALDH^{low} TEC.[17] However, when the cell cycle was analyzed using PI, a higher percentage of ALDH^{high} TEC (47.4%) was shown to be in G2/M phase, whereas 18.9% of ALDH^{low} TEC were in G2/M phase (Fig. 5a). These conflicting results led us to compare chromosomal abnormalities in ALDH^{high} TEC and ALDH^{low} TEC. Using FISH analysis of mouse chromosome 17, we observed aneuploidy in both ALDH^{high} TEC and ALDH^{low} TEC (Fig. 5b). However, ALDH^{high} TEC were shown to have a higher grade of aneuploidy, with 35% of cells containing five

© 2017 The Authors. *Cancer Science* published by John Wiley & Sons Australia, Ltd on behalf of Japanese Cancer Association.

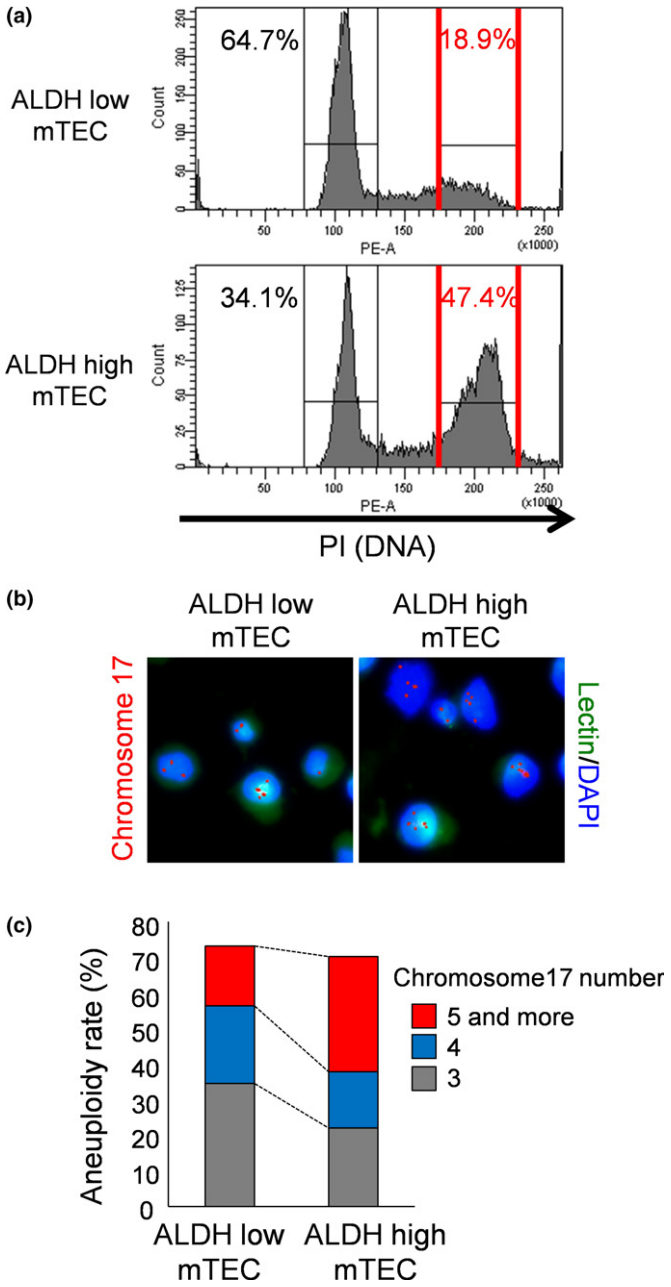

Fig. 5. High aldehyde dehydrogenase activity tumor endothelial cells (ALDH^{high} TEC) show a higher aneuploidy grade. (a) Cell cycle distribution was analyzed using propidium iodide (PI). Red line, cell population in G2/M phase. (b) FISH analysis carried out using a spectrum red-conjugated mouse chromosome-17 locus-specific probe (red spot). Nuclei are stained with DAPI (blue). (c) Quantification of chromosome 17 FISH signals in cells. Red rectangles show cells with five or more obtained signals.

or more of this chromosome number, compared with 17% of cells in ALDH^{low} TEC (Fig. 5c).

Discussion

Herein we demonstrated several findings: (i) ALDH was shown to be highly expressed in mouse TEC isolated from A375SM xenografts, and human TEC obtained from RCC patients; (ii) tumor-secreting factor (tumor CM) induced a stem-like phenotype such as stem cell marker expression, sphere-forming ability, and (iii) ALDH^{high} TEC showed resistance to the anticancer drug 5-FU *in vitro* and *in vivo*.

In the tumor microenvironment, there is heterogeneity among cancer cell populations. CSC have self-renewal potential and are considered to produce a hierarchy of cancer cells. CSC are postulated to cause heterogeneity of tumors. Moreover, they cause resistance to anticancer drugs. We previously demonstrated that TEC are also heterogeneous depending on the malignancy of the tumor. High metastatic tumor-derived TEC (HM-TEC) showed a different gene expression profile compared with low metastatic tumor-derived TEC (LM-TEC). Furthermore, HM-TEC showed a more stem cell-like phenotype and a more resistant profile to anticancer drugs (paclitaxel) with ATP-binding cassette subfamily B member 1 (ABCB1) upregulation compared with LM-TEC. In our previous study, no difference in ABCB1 expression levels was observed between ALDH^{high} and ALDH^{low} TEC[17] and, therefore, ABCB1 and ALDH may have mutually exclusive roles in drug resistance development.

Several studies have investigated the heterogeneity of the tumor endothelium.[14,24] In our study, stem-like TEC that express ALDH were sparsely distributed in tumor blood vessels, which supported EC heterogeneity. Additionally, *ALDH* expression levels were shown to be increased in HM-TEC compared with those in LM-TEC (Fig. S1), indicating that the difference in tumor microenvironment or tumor malignancy may affect ALDH expression in the EC. We reported previously that the expression levels of inflammation-related genes, such as IL-6, S100A, COX2, and biglycan, one of the damage-associated molecular pattern molecules, are also increased in HM-TEC, compared with those in LM-TEC[14,25,26] and, therefore, the changes in the inflammatory response may be responsible for the presence of ALDH^{high} TEC in the tumor microenvironment.

The presence of stem cell-like EC in pre-existing blood vessels has been previously reported. Stem cell-like EC may play important roles in pathological angiogenesis at the location of ischemia.[18] We also reported that TEC showed upregulation of certain stem cell markers and could differentiate into cells forming bone-like tissue, suggesting that they possess stem cell characteristics.[14] In addition, TEC showed high ALDH enzymatic activity, another hallmark of stem cells. ALDH is an enzyme that plays a key role in the metabolism of aldehydes. Recent studies have shown that several stem cell types, including hematopoietic stem cells and neural stem cells, possess high ALDH activity.[15] Moreover, ALDH is upregulated in several types of CSC.[27,28] Therefore, ALDH has been used as a stem cell marker.

We demonstrated that ALDH^{high} TEC possess a more proangiogenic phenotype and are more resistant to serum starvation compared with ALDH^{low} TEC.[17] EC, unlike tumor cells, have the advantages of genetic stability and absence of drug resistance development. Hence, targeting EC has been an important concept in antiangiogenic therapy. However, occasionally, the development of escape mechanisms has been reported in antiangiogenic therapy.

Because CSC are one of the causes of resistance to anticancer drugs, in the present study, we examined the involvement of stem-like TEC in drug resistance of tumor blood vessels. We reported that TEC are resistant to anticancer drugs through upregulation of P-gp/ABCB1.[13] In addition, recent studies also demonstrated that endothelial side-population cells that upregulated several ABC transporters contributed to resistance to antiangiogenic drugs.[19] Although there is increasing evidence regarding the abnormalities of TEC, the mechanisms

© 2017 The Authors. *Cancer Science* published by John Wiley & Sons Australia, Ltd on behalf of Japanese Cancer Association.

involved in these abnormalities remain to be elucidated. We previously found that tumor-secreted vascular endothelial growth factor-A induces ABCB1 mRNA upregulation in NEC by Y box-binding protein 1 activation.[13]

Thus, we propose that pre-existing EC in tumor vessels may acquire a stem cell phenotype through the effects of tumor-derived factors. To determine the regulatory mechanism of ALDH expression in TEC, we analyzed the effect of tumor-derived factors on NEC using tumor CM. Tumor CM induced the phenotype of ALDH^{high} TEC in human NEC:HMVEC such as stem marker gene upregulation, ALDH activation, and sphere-forming ability. PDGF-A upregulated ALDH expression in HMVEC, like tumor CM, suggesting that ALDH expression upregulation may be mediated by PDGF-A, at least partially. Furthermore, unlike ALDH^{low} TEC, we observed that ALDH^{high} TEC showed resistance to 5-FU. ALDH knockdown showed no direct ALDH function in TEC resistance to 5-FU. The impact of ALDH activation in CSC remains unclear. We demonstrated that ALDH^{high} TEC show a slower proliferation rate than ALDH^{low} TEC. This may represent a partial mechanism underlying the development of resistance to 5-FU in ALDH^{high} TEC.[17] However, we determined that a higher proportion of ALDH^{high} TEC was also distributed in the G2/M phase of the cell cycle, which may be explained by a higher DNA content of ALDH^{high} TEC, such as higher aneuploidy rate.

We observed that ALDH^{high} TEC demonstrated a higher grade of aneuploidy compared with ALDH^{low} TEC, suggesting possible accumulation of genetic alteration in ALDH^{high} TEC. Further studies are required to reveal the consequences of high ALDH activity in TEC.

Although further investigation is warranted, it is concluded that tumor-derived factor may induce a stem-like phenotype in EC, and these stem-like TEC may be a cause of resistance to anticancer drugs. In summary, ALDH^{high} TEC may be the cause of resistance to therapy and, therefore, contribute to tumor progression, implying that a population of pre-existing stem cells in tumor blood vessels may be an important target to overcome or prevent drug resistance.

Acknowledgments

We thank Drs Taisuke Kawamoto and Ms Suzuki for their technical assistance. The authors would like to thank Enago (www.enago.jp) for the English language review.

Disclosure Statement

Authors declare no conflicts of interest for this article.

Abbreviations

5-FU	fluorouracil
A375SM	super-metastatic human melanoma
ABC transporter	
ATP-binding cassette transporter	
ALDH	aldehyde dehydrogenase
ALDH^{high} TEC	
tumor endothelial cell containing stem-like populations with high ALDH activity	
ALDH^{low} TEC	
tumor endothelial cell with low ALDH activity	
BAAA	BODIPY-aminoacetaldehyde
CSC	cancer stem cell
EC	endothelial cell
EGM-2MV	EC growth medium for microvascular cells
HM-TEC	high metastatic tumor-derived TEC
HMVEC	human microvascular endothelial cell
hNEC	human normal endothelial cell
hTEC	human tumor endothelial cell
IL	interleukin
LM-TEC	low metastatic tumor-derived TEC
MEM	minimum essential medium
mNEC	mouse normal endothelial cell
mTEC	mouse tumor endothelial cell
MVD	microvessel density
NEC	normal endothelial cell
PDGF	platelet-derived growth factor
PE	phycoerythrin
Pgp	P-glycoprotein
PI	propidium iodide
RCC	renal cell carcinoma
STAT3	signal transducer and activator of transcription 3
TEC	tumor endothelial cell
tumor CM	tumor-conditioned medium

References

1 Folkman J. Angiogenesis: an organizing principle for drug discovery? *Nat Rev Drug Discov* 2007; **6**: 273–86.
2 Auerbach R, Akhtar N, Lewis RL, Shinners BL. Angiogenesis assays: problems and pitfalls. *Cancer Metastasis Rev* 2000; **19**: 167–72.
3 Kerbel RS, Yu J, Tran J *et al.* Possible mechanisms of acquired resistance to anti-angiogenic drugs: implications for the use of combination therapy approaches. *Cancer Metastasis Rev* 2001; **20**: 79–86.
4 Kesari S, Schiff D, Doherty L *et al.* Phase II study of metronomic chemotherapy for recurrent malignant gliomas in adults. *Neuro Oncol* 2007; **9**: 354–63.
5 Krzyzanowska MK, Tannock IF, Lockwood G, Knox J, Moore M, Bjarnason GA. A phase II trial of continuous low-dose oral cyclophosphamide and celecoxib in patients with renal cell carcinoma. *Cancer Chemother Pharmacol* 2007; **60**: 135–41.
6 Casanovas O, Hicklin DJ, Bergers G, Hanahan D. Drug resistance by evasion of antiangiogenic targeting of VEGF signaling in late-stage pancreatic islet tumors. *Cancer Cell* 2005; **8**: 299–309.
7 Maishi N, Ohga N, Hida Y *et al.* CXCR7: a novel tumor endothelial marker in renal cell carcinoma. *Pathol Int* 2012; **62**: 309–17.
8 Osawa T, Ohga N, Akiyama K *et al.* Lysyl oxidase secreted by tumour endothelial cells promotes angiogenesis and metastasis. *Br J Cancer* 2013; **109**: 2237–47.
9 Osawa T, Ohga N, Hida Y *et al.* Prostacyclin receptor in tumor endothelial cells promotes angiogenesis in an autocrine manner. *Cancer Sci* 2012; **103**: 1038–44.
10 Yamamoto K, Ohga N, Hida Y *et al.* Biglycan is a specific marker and an autocrine angiogenic factor of tumour endothelial cells. *Br J Cancer* 2012; **106**: 1214–23.
11 Hida K, Hida Y, Amin DN *et al.* Tumor-associated endothelial cells with cytogenetic abnormalities. *Cancer Res* 2004; **64**: 8249–55.
12 Akino T, Hida K, Hida Y *et al.* Cytogenetic abnormalities of tumor-associated endothelial cells in human malignant tumors. *Am J Pathol* 2009; **175**: 2657–67.
13 Akiyama K, Ohga N, Hida Y *et al.* Tumor endothelial cells acquire drug resistance by MDR1 up-regulation via VEGF signaling in tumor microenvironment. *Am J Pathol* 2012; **180**: 1283–93.
14 Ohga N, Ishikawa S, Maishi N *et al.* Heterogeneity of tumor endothelial cells: comparison between tumor endothelial cells isolated from high- and low-metastatic tumors. *Am J Pathol* 2012; **180**: 1294–307.
15 Kastan MB, Schlaffer E, Russo JE, Colvin OM, Civin CI, Hilton J. Direct demonstration of elevated aldehyde dehydrogenase in human hematopoietic progenitor cells. *Blood* 1990; **75**: 1947–50.
16 Corti S, Locatelli F, Papadimitriou D *et al.* Identification of a primitive brain-derived neural stem cell population based on aldehyde dehydrogenase activity. *Stem Cells* 2006; **24**: 975–85.

© 2017 The Authors. *Cancer Science* published by John Wiley & Sons Australia, Ltd on behalf of Japanese Cancer Association.

17 Ohmura-Kakutani H, Akiyama K, Maishi N *et al.* Identification of tumor endothelial cells with high aldehyde dehydrogenase activity and a highly angiogenic phenotype. *PLoS One* 2014; **9**: e113910.
18 Naito H, Kidoya H, Sakimoto S, Wakabayashi T, Takakura N. Identification and characterization of a resident vascular stem/progenitor cell population in preexisting blood vessels. *EMBO J* 2011; **31**: 842–55.
19 Naito H, Wakabayashi T, Kidoya H *et al.* Endothelial side population cells contribute to tumor angiogenesis and antiangiogenic drug resistance. *Cancer Res* 2016; **76**: 3200–10.
20 Akiyama K, Maishi N, Ohga N *et al.* Inhibition of multidrug transporter in tumor endothelial cells enhances antiangiogenic effects of low-dose metronomic paclitaxel. *Am J Pathol* 2015; **185**: 572–80.
21 Kondoh M, Ohga N, Akiyama K *et al.* Hypoxia-induced reactive oxygen species cause chromosomal abnormalities in endothelial cells in the tumor microenvironment. *PLoS One* 2013; **8**: e80349.
22 Silva IA, Bai S, McLean K *et al.* Aldehyde dehydrogenase in combination with CD133 defines angiogenic ovarian cancer stem cells that portend poor patient survival. *Cancer Res* 2011; **71**: 3991–4001.
23 Lin L, Hutzen B, Lee HF *et al.* Evaluation of STAT3 signaling in ALDH+ and ALDH+/CD44 + /CD24- subpopulations of breast cancer cells. *PLoS One* 2013; **8**: e82821.
24 Aird WC. Molecular heterogeneity of tumor endothelium. *Cell Tissue Res* 2009; **335**: 271–81.
25 Muraki C, Ohga N, Hida Y *et al.* Cyclooxygenase-2 inhibition causes antiangiogenic effects on tumor endothelial and vascular progenitor cells. *Int J Cancer* 2012; **130**: 59–70.
26 Maishi N, Ohba Y, Akiyama K *et al.* Tumour endothelial cells in high metastatic tumours promote metastasis via epigenetic dysregulation of biglycan. *Sci Rep* 2016; **6**: 28039.
27 Shiraishi A, Tachi K, Essid N *et al.* Hypoxia promotes the phenotypic change of aldehyde dehydrogenase activity of breast cancer stem cells. *Cancer Sci* 2016; **100**: 3983.
28 Holah NS, Aiad HA-E-S, Asaad NY, Elkhouly EA, Lasheen AG. Evaluation of the role of ALDH1 as cancer stem cell marker in colorectal carcinoma: an immunohistochemical study. *J Clin Diagn Res* 2017; **11**: EC17–23.

Supporting Information

Additional Supporting Information may be found online in the supporting information tab for this article:

Fig. S1. Aldehyde dehydrogenase (*ALDH*) mRNA expression in different tumor endothelial cells (TEC). *ALDH* expression in TEC isolated from high metastatic tumors (HM-TEC) and low metastatic tumors (LM-TEC) (*$P < 0.01$).

© 2017 The Authors. *Cancer Science* published by John Wiley & Sons Australia, Ltd on behalf of Japanese Cancer Association.